Osteoarthritis and Cartilage 21 (2013) 1895–1903

Osteoarthritis and Cartilage

OARSI OSTEOARTHRITIS RESEARCH SOCIETY INTERNATIONAL

Micromechanical mapping of early osteoarthritic changes in the pericellular matrix of human articular cartilage

R.E. Wilusz † ‡, S. Zauscher §, F. Guilak † ‡ § *

† *Department of Orthopaedic Surgery, Duke University Medical Center, United States*
‡ *Department of Biomedical Engineering, Duke University, United States*
§ *Department of Mechanical Engineering and Materials Science, Duke University, United States*

ARTICLE INFO

Article history:
Received 28 April 2013
Accepted 29 August 2013

Keywords:
Atomic force microscopy
Chondron
Type VI collagen
Scanning probe microscopy
Proteoglycan

SUMMARY

Objective: Osteoarthritis (OA) is a degenerative joint disease characterized by the progressive loss of articular cartilage. While macroscale degradation of the cartilage extracellular matrix (ECM) has been extensively studied, microscale changes in the chondrocyte pericellular matrix (PCM) and immediate microenvironment with OA are not fully understood. The objective of this study was to quantify osteoarthritic changes in the micromechanical properties of the ECM and PCM of human articular cartilage *in situ* using atomic force microscopy (AFM).

Method: AFM elastic mapping was performed on cryosections of human cartilage harvested from both condyles of macroscopically normal and osteoarthritic knee joints. This method was used to test the hypotheses that both ECM and PCM regions exhibit a loss of mechanical properties with OA and that the size of the PCM is enlarged in OA cartilage as compared to normal tissue.

Results: Significant decreases were observed in both ECM and PCM moduli of 45% and 30%, respectively, on the medial condyle of OA knee joints as compared to cartilage from macroscopically normal joints. Enlargement of the PCM, as measured biomechanically, was also observed in medial condyle OA cartilage, reflecting the underlying distribution of type VI collagen in the region. No significant differences were observed in elastic moduli or their spatial distribution on the lateral condyle between normal and OA joints.

Conclusion: Our findings provide new evidence of significant site-specific degenerative changes in the chondrocyte micromechanical environment with OA.

Introduction

Osteoarthritis (OA) is a joint disease characterized by progressive degeneration and loss of articular cartilage, ultimately resulting in severe pain and disability. In the United States, over 27 million people suffer from OA, resulting in a total annual economic burden of over 80 billion dollars[1]. While initially thought to be a disease of "normal wear and tear" associated with advanced age, it is now recognized that OA is caused by a complex interplay among biochemical, genetic, and biomechanical factors (reviewed in Ref.[2,3]) that is characterized by an imbalance between anabolic and catabolic activities in joint tissues.

Articular cartilage derives its functional mechanical properties from its extensive extracellular matrix (ECM) of type II collagen and proteoglycans. In OA, ECM degeneration is characterized by extensive proteolysis of the type II collagen network[4,5] and proteoglycans[6,7]. Relationships between these structural changes and altered cartilage mechanical properties have been observed at all stages of OA degeneration. Loss of ECM mechanical properties has been characterized at the macroscale[8–10], microscale[11,12], and nanoscale[11] in both human tissue and experimental animal models. Results at all length scales consistently show that cartilage properties in tension, compression, and shear decline with increasing disease severity.

While most investigations of changes in cartilage properties with OA focus on the macroscale properties of the ECM, many of the enzymes responsible for cartilage degradation, such as matrix metalloproteinases or aggrecanases, are synthesized and secreted by the chondrocytes[13,14]. For this reason, the microenvironment of chondrocytes may be significantly altered in early OA, before degenerative changes are apparent in the ECM at the macroscopic

* Address correspondence and reprint requests to: F. Guilak, Duke University Medical Center, Box 3093, Durham NC 27710, United States. Tel: 1-919-684-2521; Fax: 1-919-681-8490.
E-mail addresses: rebecca.wilusz@duke.edu (R.E. Wilusz), zauscher@duke.edu (S. Zauscher), guilak@duke.edu (F. Guilak).

1063-4584/$ – see front matter
http://dx.doi.org/10.1016/j.joca.2013.08.026

tissue level. Specifically, each chondrocyte in cartilage is surrounded by a narrow region known as the pericellular matrix (PCM) that together with its enclosed cell forms the functional unit known as the chondron[15]. The PCM is distinct from the bulk ECM in its biochemical composition, the predominant presence of type VI collagen[16–18], ultrastructure[19–21], and biomechanical properties[22–26]. While the exact function of this matrix region is not fully understood, growing evidence suggests that it serves to regulate the biochemical and mechanical environments of the chondrocyte[27,28]. For example, enzymes and growth factors released by chondrocytes must first pass through the PCM, where they may be retained or modified[6,29,30]. With OA, marked changes occur in the structural and biochemical profiles of the PCM. Despite local enzymatic degradation of PCM components[4,6], enlarged chondrons are prevalent in OA cartilage[31,32]. This increase in chondron volume has been attributed to the combined effects of a net increase in biosynthesis and deposition of PCM macromolecules, most notably type VI collagen[31,33], and a loosely organized ultrastructure, associated with an altered type VI collagen microfilament structure[18] that contributes to abnormal swelling. These structural changes are associated with a significant loss of the biomechanical properties of the PCM. Micropipette aspiration studies revealed that chondrons isolated from OA human cartilage exhibit Young's moduli that are 30–40% lower and permeability values that are 2–3 times greater than those of chondrons isolated from healthy tissue[22,23]. However, these previous studies involve physical extraction of the chondron from the tissue, which may result in alterations in PCM structure and properties. Furthermore, the micropipette aspiration technique cannot be used for measurement of ECM properties, and thus the extent of PCM degeneration compared to that occurring in the local ECM cannot be directly evaluated using the same measurement technique.

The objective of this study was to quantify osteoarthritic changes in the micromechanical properties of the ECM and PCM of human articular cartilage *in situ* using atomic force microscopy (AFM). Using a technique known as elastic, or force-volume mapping[26,34], AFM was used to collect arrays of indentation curves and map spatial variations in elastic modulus over ECM and PCM regions of human cartilage samples collected from macroscopically normal and early OA knee joints. This approach was used to test the hypotheses that both ECM and PCM regions experience similar losses of mechanical integrity with OA, and that the size of the PCM is enlarged in OA cartilage as compared to normal tissue.

Methods

Tissue sample preparation

Full thickness articular cartilage explants (8 mm diameter) were collected from matched sites in the load-bearing regions of both femoral condyles of eight adult human knee joints at autopsy (six females, two males; age range: 53–83 years; one joint per individual). None of the patients had a history of knee trauma or surgery and none had clinically diagnosed OA. Furthermore, no disruption of the major knee ligaments, patellar tendon, or menisci was observed in any of the knee joints. Using the Collins grading scale[35], joints were classified as macroscopically normal (Collins grade 0–1; $N = 4$) or arthritic (Collins grade 2–3; $N = 4$) based on the presence and extent of surface fibrillation, fissures, and/or focal defects on the condyles (Fig. 1). Degenerative changes were present on the medial condyle of all four OA joints, with one joint also exhibiting fibrillation on the lateral condyle [Fig. 1(C)]. Cartilage explants were wrapped in phosphate-buffered saline (PBS)-soaked gauze and frozen at −20°C for intermediate storage. In order to minimize any effects associated with freezing, cartilage samples underwent a maximum of two freeze–thaw cycles following collection[36].

To evaluate ECM and PCM mechanical properties *in situ* using AFM, cartilage samples were embedded in water-soluble embedding medium (Tissue-Tek O.C.T. Compound; Sakura Finetek USA, Torrance, CA) and were sectioned perpendicular to the articular surface in 5 μm-thick slices using a cryostat microtome (Leica CM1850; Leica Microsystems, Inc., Buffalo Grove, IL). Cryosection thickness was selected based on the diameter of the spherical probes used for AFM-based indentation. Cartilage slices were collected on glass slides and washed thoroughly with PBS to remove the water-soluble embedding medium prior to AFM testing. Cartilage slices remained in PBS at room temperature for the duration of mechanical testing. All testing was completed within 4 h of initial sectioning of cartilage samples.

Mechanical characterization via AFM-based elastic mapping

Elastic moduli were mapped quantitatively with the use of a stand-alone AFM (MFP-3D; Asylum Research, Santa Barbara, CA)[26]. For microindentation, borosilicate glass spheres (5 μm nominal diameter) were attached to the end of AFM cantilevers ($k = 7.5$ N/m; Novascan Technologies, Ames, IA). Indentation was applied by ramping the cantilever displacement at a rate of 15 μm/s until a trigger force of 750 nN was reached. On average, this force resulted in indentation depths of 0.8–1.2 μm in ECM regions and 1.8–2.2 μm in PCM regions.

PCM and ECM scan regions were located in the middle and upper deep zones of the tissue (200–400 μm from the articular surface) and selected based on microscopic examination of each cartilage section. For evaluation of PCM elastic properties, 1600 indentations were sequentially applied over 20 μm × 20 μm scan regions, encompassing cell-sized voids in the cartilage tissue section ($n = 15$–16 regions per classification). ECM elastic properties were evaluated with 16 indentations in adjacent 20 μm × 20 μm

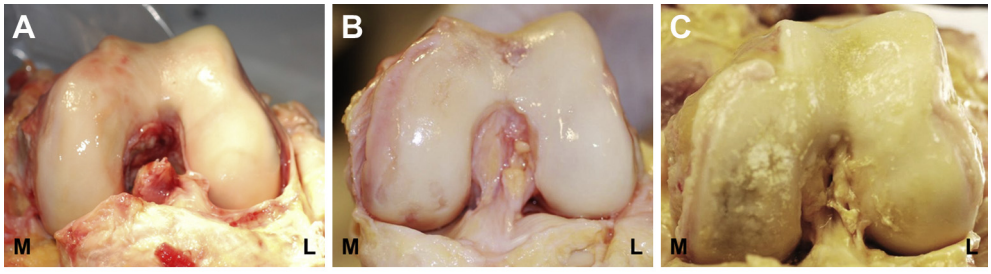

Fig. 1. Human knee joints were classified as (A) macroscopically normal or (B, C) arthritic, based on the presence and extent of surface fibrillation, fissures, and/or focal defects on the medial (M) or lateral (L) condyle. Representative knee joints for each Collins grade are shown.

regions that were visually devoid of PCM ($n = 15$–16 regions per classification).

Data evaluation

Raw data for cantilever deflection and z-piezo movement were analyzed using a custom MATLAB script (The MathWorks, Natick, MA). A modified Hertzian contact model was used to calculate tissue elastic moduli from collected force-indentation curves as described previously[37,38]. Probe-surface contact was identified using a contact point extrapolation method[39]. The Poisson's ratio was assumed to be $\nu = 0.04$ in both ECM and PCM regions based on previously published values[23,40]. Based on the Hertzian contact model, the presented modulus values can be converted to a different value of ν by multiplying by the conversion factor $(1-\nu^2)/(1-0.04^2)$, though the effect of Poisson's ratio was minimal ($\leq$12%) over $\nu = 0.04$–0.35, the range reported in the literature for cartilage PCM[23,25]. Hertzian contact mechanics provided excellent fits to the experimental data ($R^2 > 0.90$, calculated from the sum of squares of the residuals and the total sum of squares). Two-dimensional contour maps were generated of the spatial distribution of calculated elastic moduli in each scan region.

The use of a stand-alone AFM system required the use of a distance-based definition of the PCM in order to provide a consistent region for comparison across all samples tested, as outlined previously[26]. Glass contact at the center of each cell-sized void was readily apparent from the measured force-indentation curves and used to define the edge of each cell-sized void. PCM data were included for a region extending 1 μm radially from this edge to provide a consistent definition across all samples. This conservative definition likely underestimates the true extent of the PCM[17], particularly in OA cartilage where PCM thickness is increased approximately 50%[22,31], but allows for a direct comparison of the same pericellular region in all samples. For each PCM scan region, this pre-defined region contained 100–200 total indentations that were averaged to obtain the PCM elastic modulus for that region.

To quantitatively evaluate the spatial distribution of moduli in the chondrocyte microenvironment, modulus progression from the PCM inner edge to the ECM was evaluated in radial increments of 0.5 μm. In this progression, the reported PCM moduli were measured in the innermost 1 μm. Additional PCM and territorial matrix (TM) regions were assumed to extend up to 3 μm radially from the PCM inner edge[19,20]. ECM moduli reflect the properties measured in the ECM region adjacent to each PCM scan region.

Immunofluorescence for type VI collagen and histological staining

To visualize the PCM, unfixed cryosections (5 μm thick) of cartilage from the medial condyle of macroscopically normal and arthritic knee joints were labeled using immunofluorescence for type VI collagen. Sections were blocked in 10% goat serum (Invitrogen; Life Technologies, Grand Island, NY) for 30 min at room temperature. Samples were incubated with primary antibody for type VI collagen (anti-collagen type VI raised in rabbit, sc-20649; Santa Cruz Biotechnology, Inc., Santa Cruz, CA) at a 1:200 dilution in 10% goat serum for 1 h at room temperature. After three PBS washes of 5 min each, samples were incubated with secondary antibody (AlexaFluor 488 goat anti-rabbit IgG; Invitrogen) at a 1:200 dilution in 10% goat serum for 1 h in the dark at room temperature. Sections were washed three times with PBS and imaged on a confocal laser scanning microscope (LSM 510; Carl Zeiss, Inc., Thornwood, NY).

Additional cartilage explants were collected from adjacent regions on both femoral condyles for histological staining. To generate a transverse cross-section, these explants were cut in half and fixed overnight in formalin. Fixed explants were dehydrated in ethanol, infiltrated with xylene, and embedded in paraffin for sectioning. For histological staining, 10 μm-thick sections were stained with Harris Hematoxylin with glacial acetic acid (cell nuclei; Poly Scientific, Bay Shore, NC), 0.02% aqueous fast green (collagens; Sigma–Aldrich, St. Louis, MO) and Accustain Safranin-O solution (proteoglycans; Sigma–Aldrich).

Statistical analysis

For statistical analysis, each testing region was treated as an independent sample within each group, normal and OA cartilage. This assumption was made because articular cartilage exhibits significant spatial variations in properties across the joint[36] and with depth from the articular surface[41] and experiences spatial variations in loading patterns during joint motion[42]. As testing regions were selected over the entire length of the sample and were not adjacent to one another, it is highly unlikely that the regions within the same joint would have been influenced by each other or experienced the same biomechanical environment *in situ*. In this regard, cartilage mechanical properties appear to show much greater variations spatially than among individuals.

Data were log-transformed for normality in statistical analyses. Differences between ECM and PCM elastic moduli in macroscopically normal and arthritic cartilage were evaluated separately on each condyle using a two-way analysis of variance (ANOVA) (region, disease state; level of significance $\alpha = 0.05$) and Fisher's least significant difference (LSD) *post-hoc* test. As normal and OA cartilage was derived from different joints, each testing site was treated as an independent sample in these comparisons. For inter-compartment comparisons, differences in ECM and PCM elastic moduli between the medial and lateral condyles were evaluated separately for each region using a repeated measures ANOVA ($\alpha = 0.05$). Modulus progression data were evaluated separately for each disease state using a one-way ANOVA (distance; $\alpha = 0.05$) and Fisher's LSD *post-hoc* test. All data are presented as means with 95% confidence interval.

Results

Histological staining and immunofluorescence for type VI collagen

Histological staining qualitatively confirmed the presence of early degradative changes on the medial condyle of joints classified as macroscopically arthritic by Collins grade (Fig. 2). OA cartilage exhibited surface irregularities and a progressive loss of proteoglycan staining with depth as compared to macroscopically normal tissue [Fig. 2(C)]. There were no differences in the staining profiles observed on the lateral condyle between normal and arthritic joints. The articular cartilage was smooth and regular and proteoglycan staining was present throughout the depth of the tissue.

Immunofluorescence labeling illustrated distinct differences in the distribution of type VI collagen in the pericellular space between normal and OA cartilage (Fig. 3). In normal cartilage, type VI collagen was tightly localized around cell-sized voids. In contrast, expanded type VI collagen labeling occurred around cell-sized voids in OA cartilage and was faintly dispersed in ECM regions.

AFM elastic mapping of human articular cartilage

Elastic mapping of articular cartilage from the medial condyle revealed a significant loss of mechanical properties in both the PCM and ECM with OA. PCM elastic moduli in OA cartilage were reduced by 30% (96 ± 16 kPa) as compared to normal cartilage (137 ± 22 kPa; $P = 0.036$ [Fig. 4(A)]). ECM elastic moduli in OA

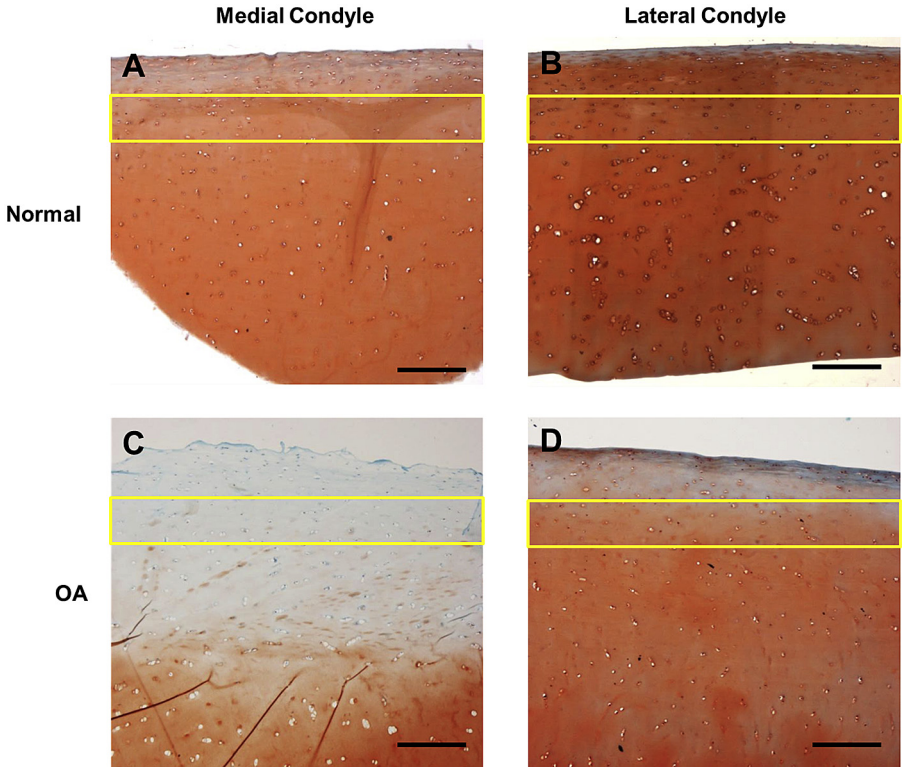

Fig. 2. Safranin-O (red, proteoglycans) and fast green (collagens, blue) staining of cartilage sections from both condyles of (A, B) macroscopically normal and (C, D) OA knee joints. Surface irregularities and a loss of proteoglycan staining are present in OA cartilage sections from the medial condyle. The AFM testing region in the middle and upper deep zones (200–400 μm from the articular surface) is labeled in each image (yellow rectangle). Scale bar = 300 μm.

cartilage were reduced by 45% (270 ± 76 kPa) as compared to normal cartilage (491 ± 112 kPa; $P < 0.001$). On the lateral condyle, no significant change in either PCM ($P = 0.814$) or ECM ($P = 0.243$) elastic moduli was observed with OA [Fig. 4(B)]. On both condyles, ECM moduli were significantly greater than PCM moduli for both normal and OA cartilage ($P < 0.001$).

Comparison between the condyles revealed distinct compartmental differences between macroscopically normal and OA knee joints. In normal joints, there was no significant difference observed in ECM moduli between the condyles ($P = 0.21$), but PCM moduli were significantly greater on the medial as compared to the lateral condyle ($P = 0.048$). In OA joints, ECM moduli were significantly reduced on the medial condyle as compared to those on the lateral condyle ($P = 0.003$) and there was no significant compartmental difference between PCM moduli ($P = 0.24$).

Spatial mapping of elastic moduli revealed alterations in the biomechanically-defined boundary of the PCM on the medial condyle with OA as compared to normal tissue. In normal cartilage, a thin matrix region exhibiting lower elastic moduli was observed immediately surrounding cell-sized voids [Fig. 5(A)]. Moduli increased with radial distance and reached ECM values within the scan region. In OA cartilage, the matrix region with lower elastic modulus was expanded and fewer regions exhibited ECM-like modulus values within the scan region [Fig. 5(B)]. This radial expansion was reflected in a shallow modulus gradient outward from the PCM inner edge [Fig. 5(C)]. Furthermore, elastic moduli failed to reach ECM-like values within a radial distance of 7.0 μm from the PCM inner edge. In contrast, ECM-like modulus values were observed at a radial distance of 6.0 μm from the PCM inner edge in normal cartilage. There were no differences observed in the PCM biomechanical footprint or outward modulus gradient on the lateral condyle between normal and OA joints [Fig. 5(D–F)].

Discussion

The findings of this study provide further evidence of significant micromechanical alterations in the articular cartilage PCM and ECM with OA. On the medial condyle, AFM-based elastic mapping revealed significant alterations in both PCM and ECM elastic moduli and their spatial distributions in OA knee joints as compared to macroscopically normal tissue. Contrary to our initial hypothesis, no significant changes were observed in either PCM or ECM moduli on the lateral condyle.

Our findings provide insight into degenerative changes in the chondrocyte micromechanical environment with OA. In comparison to previous micropipette aspiration studies on isolated chondrons, the AFM-based method utilized here has the important advantage of allowing for direct evaluation of PCM mechanical properties *in situ* while providing measurements of the local ECM mechanical properties using the same method. The observed 30% decrease in PCM elastic moduli on the medial condyle is comparable to that reported previously for comparisons of mechanically isolated chondrons from normal and OA cartilage[22,23]. Furthermore, our results suggest a direct relationship between the structural changes prevalent in OA chondrons[18,31–33] and their altered biomechanical properties.

Importantly, AFM micromechanical mapping provides a detailed measure of the spatial distribution of the tissue elastic properties in the vicinity of the chondrocyte. In agreement with the observed expansion of immunofluorescence labeling for type VI collagen in the pericellular space, the biomechanical footprint of the PCM was enlarged on the medial condyle of OA joints. Quantitative analysis of the collected elastic maps confirmed the presence of a modulus gradient outward from the PCM inner edge. On the medial condyle, a change in this gradient was observed with OA

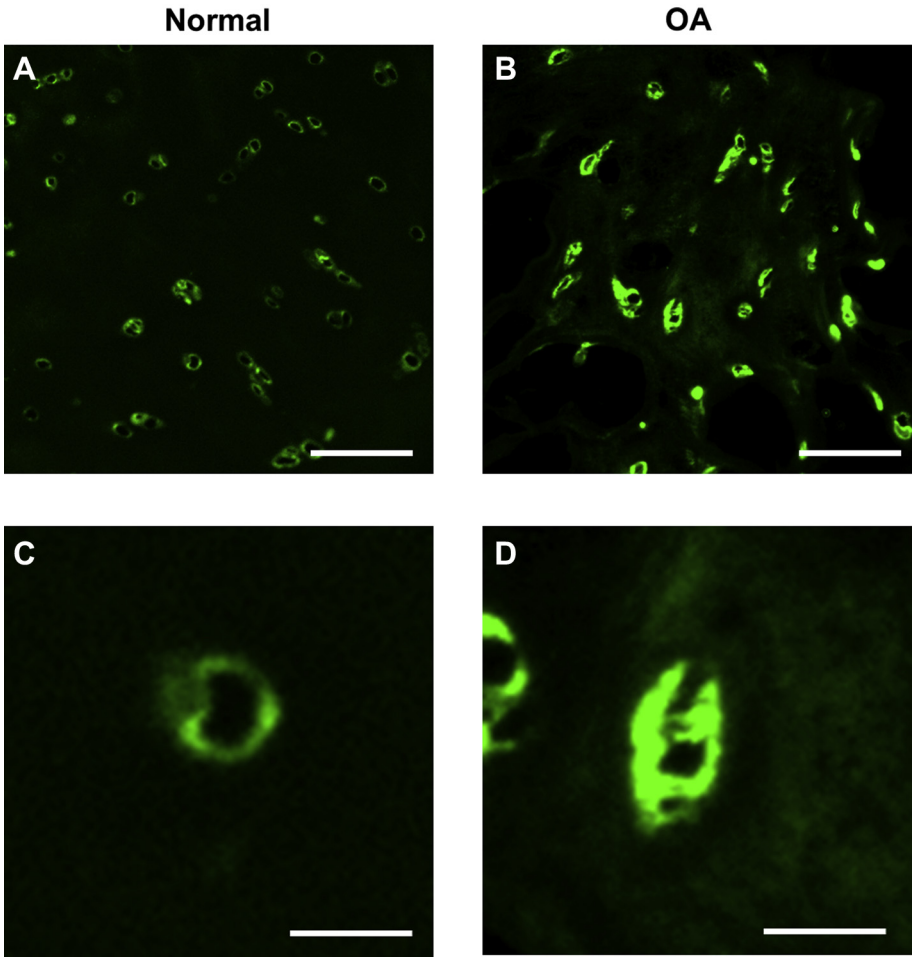

Fig. 3. (A, B) Representative images of immunofluorescence labeling of type VI collagen in cartilage from (A) macroscopically normal and (B) OA knee joints. Scale bar = 100 μm (C, D) Immunofluorescence labeling revealed expanded regions that were positive for type VI collagen in the PCM of OA cartilage. Scale bar = 25 μm.

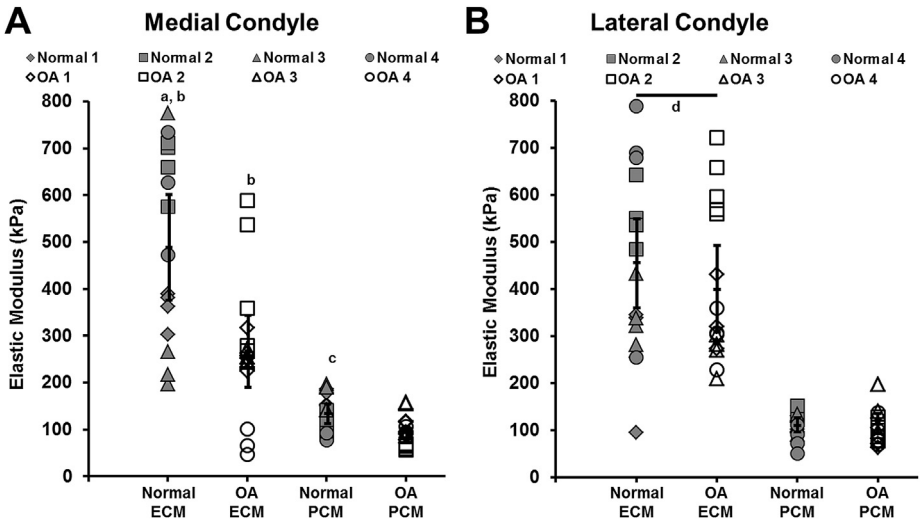

Fig. 4. Elastic moduli of cartilage ECM and PCM from the (A) medial and (B) lateral condyles of macroscopically normal (gray) and OA (white) knee joints. Testing regions from the same joint are represented by the same symbol. a: $P < 0.001$ for normal ECM moduli as compared to OA ECM moduli on the medial condyle; b: $P < 0.001$ for ECM moduli as compared to their respective PCM moduli on the medial condyle; c: $P = 0.036$ for normal PCM moduli as compared to OA PCM moduli on the medial condyle; d: $P < 0.001$ for ECM moduli as compared to their respective PCM moduli on the lateral condyle. Moduli presented individually as means with 95% confidence interval represented by the black overlaid lines ($N = 4$ knees, $n = 15–16$ regions per classification).

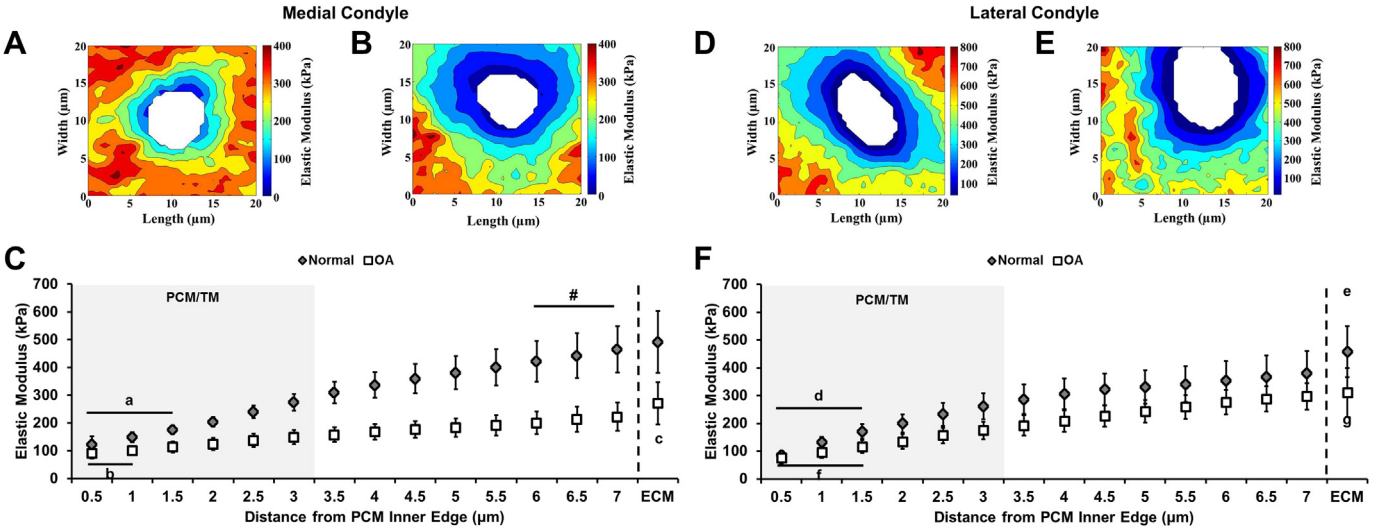

Fig. 5. Elastic mapping of PCM regions from the medial (A, B, C) and lateral condyles (D, E, F) of macroscopically normal and OA knee joints. (A, B) Representative contour maps of calculated elastic moduli for PCM scan regions of (A, D) normal and (B, E) OA cartilage from both condyles. Contour maps are presented on the same graded coloring scale and cell-sized voids are depicted in white. (C) Outward progression of elastic moduli from the PCM inner edge to the ECM of normal (gray) and OA (white) medial condyle cartilage. a: $P < 0.01$ for normal cartilage moduli within 1.5 μm of the PCM inner edge ($P < 0.001$ for 0.5 μm and 1.0 μm; $P = 0.009$ for 1.5 μm) as compared to normal moduli at a distance of 3.0 μm; b: $P < 0.05$ for OA cartilage moduli within 1.0 μm of the PCM inner edge ($P = 0.047$ for 0.5 μm; $P = 0.016$ for 1.0 μm) as compared to OA moduli at a distance of 3.0 μm; c: $P < 0.05$ for OA ECM moduli as compared to all distances in OA cartilage ($P < 0.001$ for 0.5–5.0 μm; $P = 0.001$ for 5.5 μm; $P = 0.004$ for 6.0 μm; $P = 0.018$ for 6.5 μm; $P = 0.046$ for 7.0 μm). #: Normal cartilage moduli were not significantly different from normal ECM values beginning 6.0 μm from the PCM inner edge ($P = 0.065$ for 6.0 μm; $P = 0.191$ for 6.5 μm; $P = 0.478$ for 7.0 μm). Moduli presented as means with 95% confidence interval ($N = 4$ knees, $n = 15$–16 regions per classification). (F) Outward progression of elastic moduli from the PCM inner edge to the ECM of normal (gray) and OA (white) lateral condyle cartilage. d: $P < 0.05$ for normal cartilage moduli within 1.5 μm of the PCM inner edge ($P < 0.001$ for 0.5 μm and 1.0 μm; $P = 0.017$ for 1.5 μm) as compared to normal moduli at a distance of 3.0 μm; e: $P < 0.05$ for normal ECM moduli as compared to all distances in normal cartilage ($P < 0.001$ for 0.5–5.0 μm; $P = 0.002$ for 5.5 μm; $P = 0.006$ for 6.0 μm; $P = 0.017$ for 6.5 μm; $P = 0.043$ for 7.0 μm); f: $P < 0.05$ for OA cartilage moduli within 1.5 μm of the PCM inner edge ($P < 0.001$ for 0.5 μm and 1.0 μm; $P = 0.016$ for 1.5 μm) as compared to OA moduli at a distance of 3.0 μm; g: $P < 0.05$ for OA ECM moduli as compared to all distances in OA cartilage ($P < 0.001$ for 0.5–5.5 μm; $P = 0.004$ for 6.0 μm; $P = 0.017$ for 6.5 μm; $P = 0.049$ for 7.0 μm). Moduli presented as means with 95% confidence interval ($N = 4$ knees, $n = 15$–16 regions per classification).

as compared to normal cartilage, as shown by the reduction in the slope of modulus vs distance from 54 kPa/μm in normal cartilage to 20 kPa/μm in OA cartilage. This gradient in mechanical properties likely reflects the transitional structure of this region where type II collagen fiber diameters increase with distance from the chondrocyte from the PCM to the TM to the ECM. Based on previous numerical models[43,44], the mechanical environment of the chondrocyte under static loading is not highly sensitive to the modulus of the PCM as long as the PCM modulus is more than an order of magnitude higher than that of the cell. Nonetheless, it is possible that this complex structure and gradient in properties may have significant effects under large deformations or dynamic loading, and further studies involving numerical models that account for in homogeneities in PCM properties may provide new insights into the function of this region.

Overall, the PCM moduli measured in this study fall within the range observed previously for human cartilage PCM evaluated *in situ* using AFM elastic mapping[26] but are approximately two-fold higher than those reported for isolated chondrons (96–137 kPa vs 41–66 kPa)[22,23]. This difference may reflect changes in PCM properties that occur during isolation due to damage or swelling following loss of matrix integration with the surrounding ECM. The isolation procedure can significantly alter the structural and mechanical integrity of chondrons, as evidenced by the 30- to 50-fold difference in the measured mechanical properties of enzymatically[27,45] as compared to mechanically isolated chondrons[22,23,27]. Therefore, it is possible that mechanical isolation also alters PCM properties as compared to chondrons *in situ*. This difference may also be attributed to differences in the joint of cartilage origin (i.e., hip vs knee) or to physical differences in loading with each testing modality (i.e., AFM-based indentation vs micropipette aspiration).

While macroscale degradation in articular cartilage has been extensively studied, the progression of microscale changes is not well understood. Away from the articular surface, type II collagen and aggrecan degradation epitopes are first observed in PCM/TM regions and later appear in the bulk ECM[4,6]. Furthermore, reduced type IX collagen staining has been reported in OA chondrons, reflecting a disruption of fibrillar collagen organization[5]. Since chondrocytes produce many of the catabolic enzymes implicated in OA, including aggrecanases and matrix metalloproteinases[13], local matrix degradation may originate in the PCM and progress into the local ECM. This microscale progression of chondrocyte-mediated degradation may be a significant contributor to PCM mechanical expansion and the altered cell micromechanical environment observed in this study.

In agreement with previous studies that demonstrate a significant decrease in cartilage macroscale compressive properties with the onset and progression of OA[8–10], medial condyle ECM microscale elastic moduli decreased 45% in OA cartilage as compared to macroscopically normal tissue. Contrary to our initial hypothesis, no significant change was observed in either ECM or PCM elastic moduli on the lateral condyle. In knee joints with unicompartmental OA, the mechanical properties of the "unaffected" compartment are also compromised despite the often normal macroscopic appearance of the tissue at total joint arthroplasty[46]. The lack of alteration on the lateral condyle observed in the present work is likely indicative of the relative health of our early-stage OA cartilage samples as compared to end-stage OA joints, which can exhibit widespread cartilage degeneration. Difficulties with sample preparation and testing of severely fibrillated and fissured tissue prevented end-stage OA cartilage from being included in this analysis. Overall, measured ECM moduli are in excellent agreement with macroscale modulus values previously reported for normal

and arthritic human cartilage[8,9,36] and with results demonstrating similar moduli between the medial and lateral condyles in normal joints[36]. This consistency in ECM properties at the micro- and macroscales suggests that the sample preparation methods in this study (i.e., frozen sectioning) do not have significant effects on cartilage mechanical properties.

The mechanical environment of the chondrocyte is highly dependent on the relative mechanical properties of the cell, the PCM, and its local ECM[27,43,47–49]. Thus, alterations in the mechanical properties of any of these components may result in an abnormal mechanical signaling environment in arthritic joints. While OA chondrocytes exhibit significantly higher elastic and viscoelastic properties as compared to normal chondrocytes[50], our results illustrate that the cartilage PCM and ECM exhibit significantly lower microscale elastic moduli with OA and also present evidence for alterations in the ratio of PCM to ECM properties. The PCM:ECM modulus ratio increased from 0.36 ± 0.06 in macroscopically normal medial condyle cartilage to 0.56 ± 0.13 in OA cartilage. Disruption of the relationships among cell, PCM, and ECM moduli coupled with the loss of mechanical integrity of the bulk ECM would result in significantly increased cell strains in OA as compared to normal cartilage under the same applied load. Exposure to supra-physiological strains has been associated with down-regulation of proteoglycan synthesis and increased proteoglycans release from cartilage explants *in vitro*[51–53], highlighting the potential metabolic effects of altered mechanical signaling. Such alterations in the mechanical environment can exacerbate matrix depletion in OA and contribute to the loss of cartilage matrix with disease progression.

In our study, the use of a stand-alone AFM system required the use of a distance-based definition of the PCM in order to provide a consistent region for comparison across all samples tested. While the measured PCM moduli reflect those of the region extending 1 μm radially from the edge of each cell-sized void, this conservative definition likely underestimates the true extent of the PCM[17], particularly in OA cartilage where PCM thickness is increased approximately 50%[22,31]. While microscale indentation yields moduli that reflect macroscale measurements[54], there are limits in lateral resolution associated with using micrometer-sized indenters for AFM elastic mapping, as performed here. Since the contact radius for a spherical indenter scales with tip radius and indentation depth, contact radii were larger in lower modulus PCM regions than in higher modulus ECM regions. Contact with adjacent ECM regions during indentation would result in artificial stiffening of PCM moduli at the PCM periphery. The pre-defined 1 μm PCM region was selected to minimize these effects. Further work using a hybrid AFM system integrated with an optical microscope would allow for simultaneous elastic mapping and fluorescence imaging, facilitating the use of a more precise, biochemical definition of the PCM, such as immunofluorescence labeling of type VI collagen[55] or perlecan[56,57].

Overall, our study provides further evidence of significant degenerative changes in articular cartilage at the microscale with OA. Our findings provide new insight into the micromechanical environment of the chondrocyte in the early stages of disease progression, demonstrating radial expansion of the PCM biomechanical footprint in addition to a loss in mechanical integrity. A detailed mechanical characterization of PCM alterations throughout the progression of OA could be applied to theoretical models of the chondrocyte microenvironment at multiple scales[58] to better understand alterations in cellular stress and strain to improve our understanding of the specific contributions of mechanical loading to cartilage degeneration in OA.

Funding source

This work was supported in part by a National Science Foundation Graduate Research Fellowship (REW) and National Institutes of Health grants AG15768, AR48182, AR50245, AR48852, and EB009643.

Authors' contributions

REW participated in study design and coordination, performed sample preparation, AFM elastic mapping, histological staining, immunofluorescence labeling of porcine articular cartilage, participated in study design, data analysis and interpretation, and helped draft the manuscript.

SZ participated in study coordination, provided technical and logistical support, participated in data analysis and interpretation, and helped draft the manuscript.

FG participated in study design and coordination, provided technical and logistical support, participated in data analysis and interpretation, and helped draft the manuscript.

Conflict of interest

None to declare.

Acknowledgments

The authors would like to acknowledge the Duke University Medical Center Anatomical Gifts Program for the generous donation of articular cartilage samples.

References

1. Lawrence RC, Felson DT, Helmick CG, Arnold LM, Choi H, Deyo RA, *et al*. Estimates of the prevalence of arthritis and other rheumatic conditions in the United States. Part II. Arthritis Rheum 2008;58:26–35.
2. Poole AR, Guilak F, Abramson SA. Etiopathogenesis of osteoarthritis. In: Moskowitz RW, Altman RD, Hochberg MC, Buckwalter JA, Goldberg VM, Eds. Osteoarthritis: Diagnosis and Medical/Surgical Management. Philadelphia, PA: Lippincott, Williams & Wilkins; 2007:27–49.
3. Goldring SR. The role of bone in osteoarthritis pathogenesis. Rheum Dis Clin North Am 2008;34:561–71.
4. Hollander AP, Pidoux I, Reiner A, Rorabeck C, Bourne R, Poole AR. Damage to type II collagen in aging and osteoarthritis starts at the articular surface, originates around chondrocytes, and extends into the cartilage with progressive degeneration. J Clin Invest 1995;96:2859–69.
5. Poole CA, Gilbert RT, Herbage D, Hartmann DJ. Immunolocalization of type IX collagen in normal and spontaneously osteoarthritic canine tibial cartilage and isolated chondrons. Osteoarthritis Cartilage 1997;5:191–204.
6. Plaas A, Osborn B, Yoshihara Y, Bai Y, Bloom T, Nelson F, *et al*. Aggrecanolysis in human osteoarthritis: confocal localization and biochemical characterization of ADAMTS5-hyaluronan complexes in articular cartilages. Osteoarthritis Cartilage 2007;15:719–34.
7. Lark MW, Bayne EK, Flanagan J, Harper CF, Hoerrner LA, Hutchinson NI, *et al*. Aggrecan degradation in human cartilage. Evidence for both matrix metalloproteinase and aggrecanase activity in normal, osteoarthritic, and rheumatoid joints. J Clin Invest 1997;100:93–106.
8. Armstrong CG, Mow VC. Variations in the intrinsic mechanical properties of human articular cartilage with age, degeneration, and water content. J Bone Joint Surg Am 1982;64:88–94.
9. Kleemann RU, Krocker D, Cedraro A, Tuischer J, Duda GN. Altered cartilage mechanics and histology in knee osteoarthritis: relation to clinical assessment (ICRS Grade). Osteoarthritis Cartilage 2005;13:958–63.

10. Setton LA, Elliott DM, Mow VC. Altered mechanics of cartilage with osteoarthritis: human osteoarthritis and an experimental model of joint degeneration. Osteoarthritis Cartilage 1999;7:2–14.
11. Stolz M, Gottardi R, Raiteri R, Miot S, Martin I, Imer R, *et al.* Early detection of aging cartilage and osteoarthritis in mice and patient samples using atomic force microscopy. Nat Nanotechnol 2009;4:186–92.
12. Desrochers J, Amrein MA, Matyas JR. Structural and functional changes of the articular surface in a post-traumatic model of early osteoarthritis measured by atomic force microscopy. J Biomech 2010;43:3091–8.
13. Aigner T, Zien A, Hanisch D, Zimmer R. Gene expression in chondrocytes assessed with use of microarrays. J Bone Joint Surg Am 2003;85-A(Suppl 2):117–23.
14. Song RH, Tortorella MD, Malfait AM, Alston JT, Yang Z, Arner EC, *et al.* Aggrecan degradation in human articular cartilage explants is mediated by both ADAMTS-4 and ADAMTS-5. Arthritis Rheum 2007;56:575–85.
15. Szirmai JA. Structure of cartilage. In: Engel A, Larsson T, Eds. Aging of Connective and Skeletal Tissue. Stockholm: Nordiska Bokhandelns Forlag; 1968:163–84.
16. Poole CA, Ayad S, Schofield JR. Chondrons from articular cartilage: I. Immunolocalization of type VI collagen in the pericellular capsule of isolated canine tibial chondrons. J Cell Sci 1988;90(Pt 4):635–43.
17. Youn I, Choi JB, Cao L, Setton LA, Guilak F. Zonal variations in the three-dimensional morphology of the chondron measured in situ using confocal microscopy. Osteoarthritis Cartilage 2006;14:889–97.
18. Soder S, Hambach L, Lissner R, Kirchner T, Aigner T. Ultrastructural localization of type VI collagen in normal adult and osteoarthritic human articular cartilage. Osteoarthritis Cartilage 2002;10:464–70.
19. Poole CA, Flint MH, Beaumont BW. Chondrons in cartilage: ultrastructural analysis of the pericellular microenvironment in adult human articular cartilages. J Orthop Res 1987;5:509–22.
20. Hunziker EB, Michel M, Studer D. Ultrastructure of adult human articular cartilage matrix after cryotechnical processing. Microsc Res Tech 1997;37:271–84.
21. Vanden Berg-Foels WS, Scipioni L, Huynh C, Wen X. Helium ion microscopy for high-resolution visualization of the articular cartilage collagen network. J Microsc 2012;246:168–76.
22. Alexopoulos LG, Haider MA, Vail TP, Guilak F. Alterations in the mechanical properties of the human chondrocyte pericellular matrix with osteoarthritis. J Biomech Eng 2003;125:323–33.
23. Alexopoulos LG, Williams GM, Upton ML, Setton LA, Guilak F. Osteoarthritic changes in the biphasic mechanical properties of the chondrocyte pericellular matrix in articular cartilage. J Biomech 2005;38:509–17.
24. Guilak F, Alexopoulos LG, Haider MA, Ting-Beall HP, Setton LA. Zonal uniformity in mechanical properties of the chondrocyte pericellular matrix: micropipette aspiration of canine chondrons isolated by cartilage homogenization. Ann Biomed Eng 2005;33:1312–8.
25. Kim E, Guilak F, Haider MA. An axisymmetric boundary element model for determination of articular cartilage pericellular matrix properties in situ via inverse analysis of chondron deformation. J Biomech Eng 2010;132. 031011.
26. Darling EM, Wilusz RE, Bolognesi MP, Zauscher S, Guilak F. Spatial mapping of the biomechanical properties of the pericellular matrix of articular cartilage measured in situ via atomic force microscopy. Biophys J 2010;98:2848–56.
27. Knight MM, Ross JM, Sherwin AF, Lee DA, Bader DL, Poole CA. Chondrocyte deformation within mechanically and enzymatically extracted chondrons compressed in agarose. Biochim Biophys Acta 2001;1526:141–6.
28. Guilak F, Alexopoulos LG, Upton ML, Youn I, Choi JB, Cao L, *et al.* The pericellular matrix as a transducer of biomechanical and biochemical signals in articular cartilage. Ann N Y Acad Sci 2006;1068:498–512.
29. Echtermeyer F, Bertrand J, Dreier R, Meinecke I, Neugebauer K, Fuerst M, *et al.* Syndecan-4 regulates ADAMTS-5 activation and cartilage breakdown in osteoarthritis. Nat Med 2009;15:1072–6.
30. Macri L, Silverstein D, Clark RA. Growth factor binding to the pericellular matrix and its importance in tissue engineering. Adv Drug Deliv Rev 2007;59:1366–81.
31. Lee GM, Paul TA, Slabaugh M, Kelley SS. The incidence of enlarged chondrons in normal and osteoarthritic human cartilage and their relative matrix density. Osteoarthritis Cartilage 2000;8:44–52.
32. Poole CA, Matsuoka A, Schofield JR. Chondrons from articular cartilage. III. Morphologic changes in the cellular microenvironment of chondrons isolated from osteoarthritic cartilage. Arthritis Rheum 1991;34:22–35.
33. Hambach L, Neureiter D, Zeiler G, Kirchner T, Aigner T. Severe disturbance of the distribution and expression of type VI collagen chains in osteoarthritic articular cartilage. Arthritis Rheum 1998;41:986–96.
34. Elkin BS, Azeloglu EU, Costa KD, Morrison 3rd B. Mechanical heterogeneity of the rat hippocampus measured by atomic force microscope indentation. J Neurotrauma 2007;24:812–22.
35. Collins DH, McElligott TF. Sulphate ($^{35}SO_4$) uptake by chondrocytes in relation to histological changes in osteoarthritic human articular cartilage. Ann Rheum Dis 1960;19:318–30.
36. Athanasiou KA, Rosenwasser MP, Buckwalter JA, Malinin TI, Mow VC. Interspecies comparisons of in situ intrinsic mechanical properties of distal femoral cartilage. J Orthop Res 1991;9:330–40.
37. Harding JW, Sneddon IN. The elastic stresses produced by the indentation of the plane surface of a semi-infinite elastic solid by a rigid punch. Math Proc Camb Philos Soc 1945;41:16–26.
38. Darling EM, Zauscher S, Guilak F. Viscoelastic properties of zonal articular chondrocytes measured by atomic force microscopy. Osteoarthritis Cartilage 2006;14:571–9.
39. Guo S, Akhremitchev BB. Packing density and structural heterogeneity of insulin amyloid fibrils measured by AFM nanoindentation. Biomacromolecules 2006;7:1630–6.
40. Athanasiou KA, Agarwal A, Muffoletto A, Dzida FJ, Constantinides G, Clem M. Biomechanical properties of hip cartilage in experimental animal models. Clin Orthop Relat Res 1995:254–66.
41. Schinagl RM, Gurskis D, Chen AC, Sah RL. Depth-dependent confined compression modulus of full-thickness bovine articular cartilage. J Orthop Res 1997;15:499–506.
42. Coleman JL, Widmyer MR, Leddy HA, Utturkar GM, Spritzer CE, Moorman 3rd CT, *et al.* Diurnal variations in articular cartilage thickness and strain in the human knee. J Biomech 2013;46:541–7.
43. Guilak F, Mow VC. The mechanical environment of the chondrocyte: a biphasic finite element model of cell-matrix interactions in articular cartilage. J Biomech 2000;33:1663–73.
44. Kim E, Guilak F, Haider MA. The dynamic mechanical environment of the chondrocyte: a biphasic finite element model of cell-matrix interactions under cyclic compressive loading. J Biomech Eng 2008;130. 061009.
45. Guilak F, Jones WR, Ting-Beall HP, Lee GM. The deformation behavior and mechanical properties of chondrocytes in articular cartilage. Osteoarthritis Cartilage 1999;7:59–70.

46. Obeid EM, Adams MA, Newman JH. Mechanical properties of articular cartilage in knees with unicompartmental osteoarthritis. J Bone Joint Surg Br 1994;76:315–9.
47. Baer AE, Laursen TA, Guilak F, Setton LA. The micromechanical environment of intervertebral disc cells determined by a finite deformation, anisotropic, and biphasic finite element model. J Biomech Eng 2003;125:1–11.
48. Choi JB, Youn I, Cao L, Leddy HA, Gilchrist CL, Setton LA, *et al*. Zonal changes in the three-dimensional morphology of the chondron under compression: the relationship among cellular, pericellular, and extracellular deformation in articular cartilage. J Biomech 2007;40:2596–603.
49. Julkunen P, Wilson W, Jurvelin JS, Korhonen RK. Composition of the pericellular matrix modulates the deformation behaviour of chondrocytes in articular cartilage under static loading. Med Biol Eng Comput 2009;47:1281–90.
50. Trickey WR, Lee GM, Guilak F. Viscoelastic properties of chondrocytes from normal and osteoarthritic human cartilage. J Orthop Res 2000;18:891–8.
51. DiMicco MA, Patwari P, Siparsky PN, Kumar S, Pratta MA, Lark MW, *et al*. Mechanisms and kinetics of glycosaminoglycan release following in vitro cartilage injury. Arthritis Rheum 2004;50:840–8.
52. Quinn TM, Allen RG, Schalet BJ, Perumbuli P, Hunziker EB. Matrix and cell injury due to sub-impact loading of adult bovine articular cartilage explants: effects of strain rate and peak stress. J Orthop Res 2001;19:242–9.
53. Stolberg-Stolberg JA, Furman BD, Garrigues NW, Lee J, Pisetsky DS, Stearns NA, *et al*. Effects of cartilage impact with and without fracture on chondrocyte viability and the release of inflammatory markers. J Orthop Res 2013;31:1283–92.
54. Stolz M, Raiteri R, Daniels AU, VanLandingham MR, Baschong W, Aebi U. Dynamic elastic modulus of porcine articular cartilage determined at two different levels of tissue organization by indentation-type atomic force microscopy. Biophys J 2004;86:3269–83.
55. Wilusz RE, Defrate LE, Guilak F. Immunofluorescence-guided atomic force microscopy to measure the micromechanical properties of the pericellular matrix of porcine articular cartilage. J R Soc Interface 2012;9:2997–3007.
56. Wilusz RE, Defrate LE, Guilak F. A biomechanical role for perlecan in the pericellular matrix of articular cartilage. Matrix Biol 2012;31:320–7.
57. Sanchez-Adams J, Wilusz RE, Guilak F. Atomic force microscopy reveals regional variations in the micromechanical properties of the pericellular and extracellular matrices of the meniscus. J Orthop Res 2013;31:1218–25.
58. Halloran JP, Sibole S, van Donkelaar CC, van Turnhout MC, Oomens CW, Weiss JA, *et al*. Multiscale mechanics of articular cartilage: potentials and challenges of coupling musculoskeletal, joint, and microscale computational models. Ann Biomed Eng 2012;40:2456–74.